Electronic Supplementary Information

Precisely NIR-II-activated and pH-responsive cascade catalytic nanoreactor for controlled drug release and self-enhanced synergetic therapy

Peng Hu, Shuang Zhao,* Jiahua Shi*, Fan Li, Shaochen Wang, Ying Gan, Lei Liu, Shuling Yu

Key Laboratory of Natural Medicine and Immune-Engineering of Henan Province, Henan University, Kaifeng, Henan 475004, P. R. China

***Corresponding Authors**

E-mail: szhao@henu.edu.cn. (S. Zhao)

E-mail: sjiahua@henu.edu.cn (J. Shi)

Experimental section

Materials

Pluronic® F127, dopamine hydrochloride (98%, AR), tris(hydroxymethyl) aminomethane (TRIS, 99.9%), 1,3,5-trimethylbenzene (TMB, 97%), mercaptosuccinic acid (MSA), doxorubicin hydrochloride (DOX, 98%), 2',7'-Dichlorodihydrofluorescein diacetate (DCFH-DA), glucose oxidase (GOx), Calcein AM, and propidium iodide (PI) were purchased from the Aladdin Reagent Co. Ltd. (Shanghai, China). H_2O_2 detection kit, DMEM medium, phosphate buffer (PBS), saline, and 4,6-diamidino-2-phenylindole (DAPI) were obtained from Solarbio Technology Co., Ltd (Beijing, China). All reagents were used as obtained without further purification.

Characterization

The morphology and size of various nanoparticles were recorded by transmission electron microscope (TEM, JEOL-2010, 200 kV). Dynamic light scattering (DLS) measurements were used to characterize the hydrodynamic diameter and surface charges on a Zetasizer Nano ZS (Malvern Instruments Ltd., UK). The UV-Vis-NIR absorption were recorded by a Shimadzu UV-3600 (Shimadzu Co., Japan). Fourier transform infrared (FTIR) spectra were monitored by PerkinElmer 580B IR (PerkinElmer, USA) spectrophotometer. The cells fluorescence imaging was performed on a fluorescence microscope (Leica, DMi8).

Synthesis of hollow mesoporous polydopamine (HMPDA)

HMPDA was synthesized according to the method reported previously by our group with slight modification[1]. Briefly, 0.30 g F127 and 500 μL 1,3,5-trimethylbenzene (TMB) were added to a mixture of H_2O (25 mL) and ethanol (25 mL)

and stirred continuously at room temperature for 2 h. Then, 15 mg dopamine hydrochloride and 4 mL aqueous solution containing 90 mg Tris(hydroxymethyl)aminomethane (Tris) were successively added to the above solution. After 24 h, the precipitate was obtained by centrifugation and then washed with a mixture of ethanol and acetone (2:1 v/v). The final product was re-dispersed in deionized water for further use.

Synthesis of HMPDA@$Cu_{2-x}Se$ (HMPC)

Ultra-small $Cu_{2-x}Se$ was synthesized on basis of the method reported previously with slight modifications[2, 3]. Firstly, 10 mL $NaBH_4$ (0.3 mmol) aqueous solution were injected to a bottle containing 0.1 mmol Se powder and stirred under the protection of N_2 to obtain selenium precursor solution. After the solution was clarified, 5 mL mixed solution of $CuCl_2 \cdot 2H_2O$ (0.2 mmol) and mercaptosuccinic acid (MSA, 1.33 mmol) was injected into the above solution. The solution turned dark green immediately, demonstrating the formation of $Cu_{2-x}Se$. The reaction was continued for 2.5 h and the obtained $Cu_{2-x}Se$ nanomaterial was purified by dialyzing in water for 24 h to remove excessive MSA. Finally, the dialyzed $Cu_{2-x}Se$ solution was lyophilized, re-dispersed in deionized water and stored at 4 ^{o}C for further use.

In order to bind ultra-small $Cu_{2-x}Se$ to HMPDA, 10 mg HMPDA was added to 10 mL $Cu_{2-x}Se$ solution (1 mg mL^{-1}) and stirred continuously at room temperature for 12 h. After centrifugation, the precipitates were washed with deionized water and stored at 4 ^{o}C for further use.

Drug loading (DOX and GOx) performance

For DOX loading , HMPDA@$Cu_{2-x}Se$ (4 mg) and DOX·HCl (2, 4, 8, 12, and 16 mg) were mixed in deionized water and stirred in dark for 24 h at room temperature. The products (denoted as HMPC-D) were obtained by centrifugation and washed with deionized water for several times. All supernatants were collected and the absorbances at 480 nm were measured to determine the loading efficiency of DOX.

For GOx loading, 20 mg HMPC-D and 5 mg GOx were mixed in 20 mL deionized water and stirred for 6 h. The prepared product of HMPDA@$Cu_{2-x}Se$-DOX-GOx (denoted as HMPC-D/G) was centrifuged, washed with deionized water for three times and restored in PBS for further use. The loading content of GOx was tested according to the instructions of bicinchoninic acid (BCA) protein quantification kit. The drug-loading efficiency (LE) of DOX or GOx was calculated as the following equation:

$$\text{Loading efficiency (wt \%)} = \frac{mass\ of\ total\ drug - mass\ of\ drug\ in\ supernatant}{mass\ of\ total\ drug} \times 100\%$$

For better control over the drug release, organic phase-change materials (PCM), 1-tetradecanol (1-TD) was chosen as the gatekeeper to encapsulate the drugs. Briefly, 10 mg 1-TD was dissolved in 20 mL deionized water at 45 °C. Then, 20 mg HMPC-D/G in 10 mL aqueous solution was added and stirred at 45 °C for 2 h. After cooling to room temperature, the unreacted 1-TD was removed by centrifugation to obtain the final product (HMPC-D/G@PCM).

Photothermal performance

To study the photothermal effect of the synthesized HMPC-D/G@PCM, different concentrations of HMPC-D/G@PCM solution (HMPDA: 0, 50, 100, 200, and 400 μg

mL^{-1}) were irradiated with an 808/1064 nm NIR laser (1.0 W cm^{-2}) for 10 min, and the temperature of the solution was recorded by a thermometer every 30 s. Meanwhile, real-time thermal images were monitored by an infrared imaging camera. Besides, the temperature variation of HMPC-D/G@PCM (MPDA: 200 μg mL^{-1}) under different laser power densities (0, 0.75, 1, 1.5, 2 W cm^{-2}) were also studied respectively by the same method. Furthermore, the photothermal stability of the as-obtained HMPC-D/G@PCM nanomaterial was detected through 5 cycles of laser on/off irradiation operation (one cycle includes laser on for 10 min and then natural cooling to room temperature).

NIR/pH-responsive release of the loaded drugs

To investigate the NIR- and pH-controlled release behavior of the as-synthesized HMPC-D/G@PCM, four experimental groups were conducted as follows: (1) pH 7.4，without NIR; (2) pH 7.4, with NIR (1064 nm) laser (1.5 W cm^{-2}, 10 min); (3) pH 5.0, without NIR; and (4) pH 5.0, with NIR (1064 nm, 1.5 W cm^{-2}, 10 min). In detail, 2 mg HMPC-D/G@PCM dispersed in 3 mL PBS (pH: 7.4, 5.0, respectively) was dialyzed in 20 mL water and shaken at 37 °C. At specified time points, 2 mL dialysis solution was taken from the solution and 2 mL fresh PBS was added to the buffer at the same time. For the NIR group, 10 min of NIR irradiation was applied in every time stage of drug release. The concentration of released DOX and GOx were determined by UV-vis absorbance and BCA detection kit, respectively.

In vitro ·OH generation

3,3′,5,5′-tetramethylbenzidine (TMB) was used as a colorimetric probe to detect

the production of •OH. Briefly, 200 μL H_2O_2 solution (0, 1, 5, 10 mM) and 100 μL TMB solution (4 mM) were successively added to 2 mL HMPDA@$Cu_{2-x}Se$ solution (400 μg mL^{-1}), respectively. Then, the mixture was exposed to 1064 nm laser for 10 min. After cooling to room temperature, the mixture was centrifuged and the supernatants were collected. The absorbance of the supernatants at 652 nm were monitored by UV–vis spectroscopy. Besides, •OH generation under various HMPDA@$Cu_{2-x}Se$ concentrations (50, 100, 200, 400 μg mL^{-1}) and H_2O_2 solution (10 mM) was evaluated by the same method. Moreover, terephthalic acid (TA) was selected as a fluorescence probe for specific detection of •OH radicals. HMPC-D/G@PCM nanoparticles (HMPDA: 400 μg mL^{-1}), glucose (4 mg mL^{-1}) and TA (6 mM) were mixed in water for 2 h. The generation of •OH radicals with or without 1064 nm laser irradiation was detected by measuring the fluorescence emission of the mixed solution at the excitation of 315 nm.

Intracellular •OH was detected using 2,7-Dichlorodihydrofluorescein diacetate (DCFH-DA) as the ROS detection probe. HepG2 cells were seeded in 6-well plates and incubated at 37℃ for 24 h. Then, the cultured HepG2 cells were divided into 8 groups and treated accordingly: (1) PBS; (2) NIR; (3) DOX-GOx; (4) DOX-GOx+NIR; (5) HMPDA@$Cu_{2-x}Se$; (6) HMPDA@$Cu_{2-x}Se$+NIR; (7) HMPC-D/G@PCM; (8) HMPC-D/G@PCM +NIR. After incubating for another 6 h, the medium was removed and the cells were washed with PBS buffer. Then, 100 μL fresh medium containing 10 μL of DCFH-DA (2 mg mL^{-1}) was added and the cells were incubated for 15 min. Subsequently, the fluorescence images of 2,7-dichlorofluorescein (DCF) (λex = 480

nm, λem = 525 nm) were observed using an inverted fluorescent microscope.

In vitro synergistic reactions

To demonstrate the promotion of NIR irradiation towards the Fenton reaction of the synthesized HMPDA@$Cu_{2-x}Se$ nanomaterial, H_2O_2 (200 μL, 10 mM), TMB solution (100 μL, 4 mM), and HMPDA@$Cu_{2-x}Se$ solution (2 mL, 400 μg mL^{-1}) were mixed and stirred for 10 min under 1064 nm laser irradiation. Then, the supernatant was collected by centrifugation and the absorbance at 652 nm was detected.

To verified the effect of GOx catalysis on the production of •OH, HMPC-D/G@PCM nanoparticles were dissolved in PBS buffer containing different concentrations of glucose (0.1, 0.2, 0.5, 1.0, 2.0, and 4.0 mg mL^{-1}). Then, TMB (4 mM) was added to the above solution and exposed to 1064 nm laser to demonstrate the synergistic reaction. For comparation, a group without NIR laser irradiation was conducted in glucose solution (1 mg mL^{-1}).

GOx catalytic activity was evaluated by monitoring the glucose consumption and the reaction products of gluconic acid and hydrogen peroxide (H_2O_2). 3,5-dinitrosalicylic acid (DNS) method was used to detect the glucose consumption. Briefly, 1 mL HMPC-D/G@PCM solution (HMPDA: 200 μg mL^{-1}) was mixed with 1 mL glucose solution (4 mg mL^{-1}). At specific time points, the mixture was centrifuged and the supernatants were collected. Afterwards, 3 mL DNS reagent was mixed with the obtained supernatants above and bathed in boiling water for 5 min. Finally, the concentration of remaining glucose in supernatants was determine by detecting the absorbance at 540 nm. Besides, the effect of NIR laser on the consumption of glucose

was monitored by irradiating the mixture of HMPC-D/G@PCM and glucose solution by 1064 nm laser before collecting the supernatants. The remaining amount of glucose was evaluated by the same assay.

The production of gluconic acid and H_2O_2 was detected as the following methods. For pH variation, 1 mL HMPC-D/G@PCM (HMPDA: 200 μg mL^{-1}) was mixed homogeneously with 1 mL glucose solution (4 mg mL^{-1}). Gluconic acid production was confirmed by evaluating the time-dependent pH changes with a pH meter. For the generation of H_2O_2, the mixture of HMPC-D/G@PCM (1 mL, HMPDA: 200 μg mL^{-1}) and glucose solution (4 mg mL^{-1}) was shock at 37 ^oC for various times and the supernatants were collected. The concentration of H_2O_2 in the supernatants was detected with a H_2O_2 detection kit according to the manual provided with the reagents.

Cellular uptake

HepG2 cells were seeded in confocal petri dishes (5000 cells per well) and incubated for 24 h. Afterwards, 1 mL DMEM medium containing HMPC-D/G@PCM (200 μg mL^{-1}) was added and cultured for another 1, 3, and 6 h, respectively. Then, the cells were washed with PBS and stained with 4′,6-diamidino-2-phenylindole (DAPI). After incubating for another 15 min, the fluorescent images were recorded by confocal laser scanning microscope (CLSM). In addition, in order to demonstrate the effect of NIR irradiation on cellular uptake and drug release, NIR irradiation was employed on the groups consistent with that without laser exposure (5 min, 1.5 W cm^{-2}) The other conditions remained unchanged and the fluorescence images were detected by CLSM accordingly.

In vitro cytotoxicity

Standard MTT assay was used to evaluate the cytotoxicity of HMPDA@$Cu_{2-x}Se$ to HepG2, 7702 and 293T cells. Briefly, HepG2 cells were seeded in 96-well plates at a density of 10^4 cells per well and incubated at 37 ^oC for 24 h. Then, original medium was replaced by fresh medium containing different concentrations of HMPDA@$Cu_{2-x}Se$ (0, 50, 100, 200, and 400 μg mL^{-1}) and incubated for another 24 h. After washing by PBS, 100 μL fresh medium containing 10 μL MTT was added and the cells were incubated for another 4 h. Finally, the absorbance of each well at 490 nm was recorded using a microplate reader. To evaluate the cellular compatibility of HMPDA@$Cu_{2-x}Se$ NPs on normal cells, 7702 and 293T cells were subjected to the same tests as described above, respectively.

To prove the in vitro synergistic therapy of the synthesized HMPC-D/G@PCM, HepG2 cells were cultured and treated with different conditions accordingly: (1) control (±NIR), (2) DOX (±NIR), (3) GOx (±NIR), (4) DOX+GOx (±NIR), (5) HMPC-D@PCM (HMPDA@$Cu_{2-x}Se$-DOX@PCM) (±NIR), (6) HMPC-G@PCM (HMPDA@$Cu_{2-x}Se$-GOx@PCM) (±NIR), (7) HMPC-D/G@PCM (HMPDA@$Cu_{2-x}Se$-DOX/GOx@PCM) (±NIR). Among them, the cells in the NIR group were irradiated by NIR laser (1064 nm, 1.5 Wcm^{-2}, 5 min) after 4 h incubated with the synthesized nanomaterials and then cultured for another 20 h before the employment of MTT assay.

Live/Dead Assay

The live/dead staining kits were conducted to further evaluate cancer cell ablation

ability of the synthesized nanomaterials under NIR laser irradiation. HepG2 cells were incubated at different conditions as follows: (1) Control, (2) NIR, (3) DOX, (4) GOx, (5) HMPDA@$Cu_{2-x}Se$, (6) HMPDA@$Cu_{2-x}Se$+NIR, (7) HMPC-D/G@PCM, (8) HMPC-D@PCM+NIR, (9) HMPC-D/G@PCM+NIR. For the groups with NIR irradiation, 1064 nm laser (1.5 W cm^{-2}, 5 min) was employed after incubating the cells with the corresponding nanomaterials for 6 h. After that, the cells were washed by PBS buffer and then co-stained with 5 μM calcein AM and 10 μM PI at 37 °C for 20 min. Eventually, fluorescence images were obtained under an inverted fluorescence microscope.

In vivo biocompatibility

All the animal experiments were carried out in accordance with the Regulations for the Administration of Affairs Concerning Experimental Animals of the People's Republic of China and approval of the Animal Management and Ethics Committee of Henan University (Kaifeng, China) to ensure animal welfare during the experiments. The mice used for animal experiments were obtained from Huaxing Experimental Animal Center (Zhengzhou, China).

Red blood cells were separated with plasma by centrifugation at 2000 r min^{-1} for 10 min, washed with 0.9 % NaCl solution until the supernatant is colorless and then mixed with 1 mL of water (negative control), saline (positive control) and various concentrations of HMPC-D/G@PCM solution (50, 100, 200, 400, 800 μg mL^{-1}), respectively. After incubating at 37 °C for 3 h, the supernatants were collected by centrifugation and the absorbance at 540 nm was recorded using a UV-vis

spectrophotometer. The percentage of hemolysis was calculated by the following equation:

$$\text{Hemolysis (\%)} = (\text{As- An})/(\text{Ap-An}) \times 100\ \%$$

where As, An, and Ap are the absorbance of samples, the negative control, and positive control, respectively.

To further ensure in vivo application of the synthesized nanomaterial, more complete toxicology experiments were carried out on ICR healthy mice. Different groups of materials (saline, HMPDA@$Cu_{2-x}Se$ (200 μg), HMPC-D/G@PCM (200 μg and 400 μg)) were injected into mice via tail vein. Blood was taken from the orbits of each group of mice after 4 weeks of feeding. The blood routine, serum biochemical indexes, organ coefficients, and histopathological evaluation of major organs were detected.

In vivo distribution and photothermal imaging

The fluorescence imaging was performed on H22 tumor-bearing Kunming mice to detect the in vivo distribution of HMPDA@$Cu_{2-x}Se$. Firstly, HMPDA@$Cu_{2-x}Se$ was labeled by a near-infrared fluorescence dye (NIR-797). Briefly, NIR-797 in DMSO (1 mg mL^{-1}) was mixed with HMPDA@$Cu_{2-x}Se$ and HMPC-D/G@PCM aqueous solution. Then, 20 μL triethylamine was added and the mixture was stirred continuously for 24 h to obtain the NIR-797 labeled HMPDA@$Cu_{2-x}Se$ and HMPC-D/G@PCM nanomaterials, respectively. When the tumor volume reached about 300 mm^3, the mice were intravenously injected with 200 μL saline solution of NIR-797 labeled HMPDA@$Cu_{2-x}Se$ and HMPC-D/G@PCM (HMPDA: 1 mg mL^{-1}) nanomaterials,

respectively. The fluorescence imaging of mice was performed at different times (1, 2, 4, 8, 12, and 24 h at post-injection) using in vivo imaging system with an excitation wavelength of 740 nm and an emission wavelength of 790 nm. After 48 h, the mice were dissected and the main organs were imaged.

Besides, the photothermal imaging performance was evaluated. The tumor-bearing mice were intravenously injected with saline, HMPDA@$Cu_{2-x}Se$, HMPC-D/G@PCM (HMPDA: 1 mg mL^{-1}). After 12 h injection, the mice were irradiated with 1064 nm light (1.5 W cm^{-2}) for 10 min, and the thermal images were taken every minute with an infrared thermal imaging camera.

In vivo antitumor effect and histological analysis

When the tumor volume of mice reached about 100 mm^3, the mice were randomly divided into 9 groups (n=4): (1) control; (2) NIR; (3) GOx, (4) HMPDA@$Cu_{2-x}Se$; (5) HMPDA@$Cu_{2-x}Se$+NIR; (6) DOX; (7) HMPC-D/G@PCM; (8) HMPC-D@PCM +NIR; (9) HMPC-D/G@PCM+NIR. Then, the in vivo antitumor efficiency of the obtained nanomaterials was evaluated through intravenous injection (DOX 5 mg kg^{-1}, GOx 2 mg kg^{-1}, 200 μL, the equivalent concentration for HMPDA was about 200 μg). Among them, the mice requiring NIR irradiation were irradiated with 1064 nm laser for 6 min after the injection of corresponding nanoparticles for 12 h. Tumor volume was calculated according to the following formula: volume (V) = length × $width^2/2$ and the body weight were recorded every two days. After 14 days, the mice were sacrificed and the tumors were removed for photographs. Then, the major organs and tumors were preserved in 4 % formalin for further H&E staining.

References:

1. K. Lin, Y. Gan, P. Zhu, S. Li, C. Lin, S. Yu, S. Zhao, J. Shi, R. Li and J. Yuan, Nanotechnology, 2021, 32, 285602.

2. T. Wang, H. Zhang, H. Liu, Q. Yuan, F. Ren, Y. Han, Q. Sun, Z. Li and M. Gao, 2020, 30, 1906128.

3. H. Zhang, T. Wang, H. Liu, F. Ren, W. Qiu, Q. Sun, F. Yan, H. Zheng, Z. Li and M. Gao, Nanoscale, 2019, 11, 7600-7608.

Supplementary figures

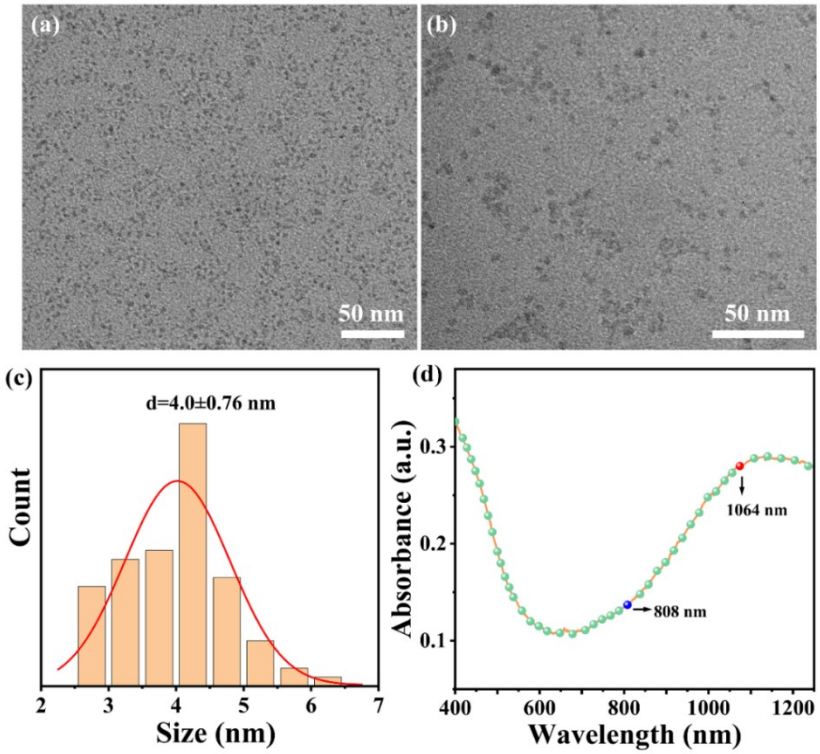

Fig. S1 (a, b) TEM images, (c) Histogram of the particle size distribution, and (d) UV-visible near-infrared (UV–Vis-NIR) spectrum of the synthesized $Cu_{2-x}Se$ nanoparticles.

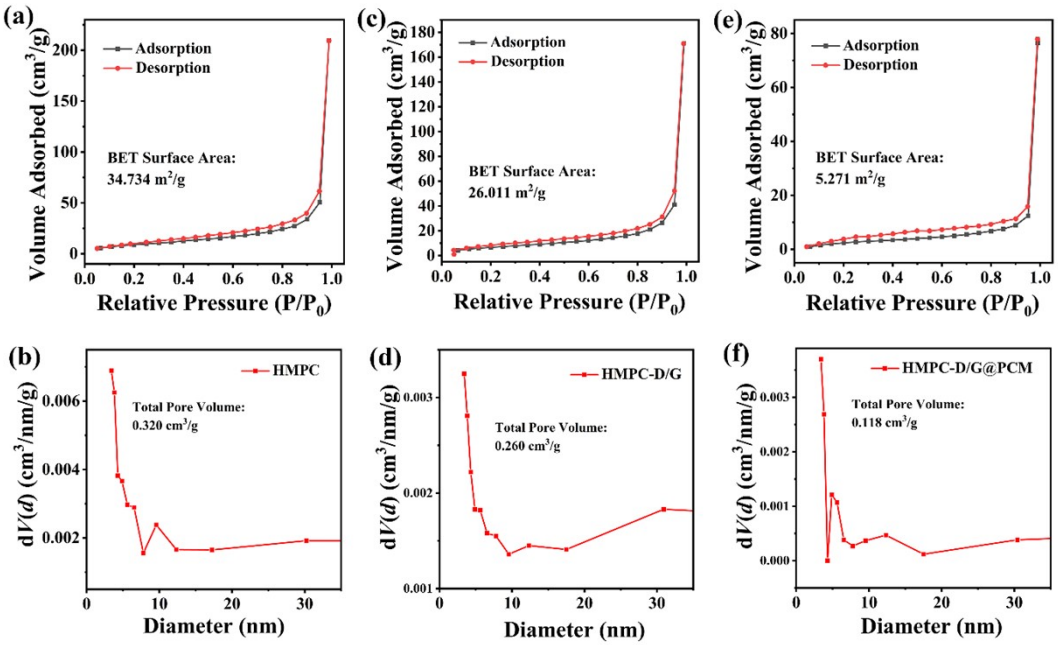

Fig. S2 Nitrogen absorption/desorption isotherms (a, c, e) and corresponding pore size distribution obtained by the BJH desorption method (b, d, f) of (a, b) HMPDA@$Cu_{2-x}Se$ (HMPC), (c, d) HMPC-D/G, and (e, f) HMPC-D/G@PCM, respectively.

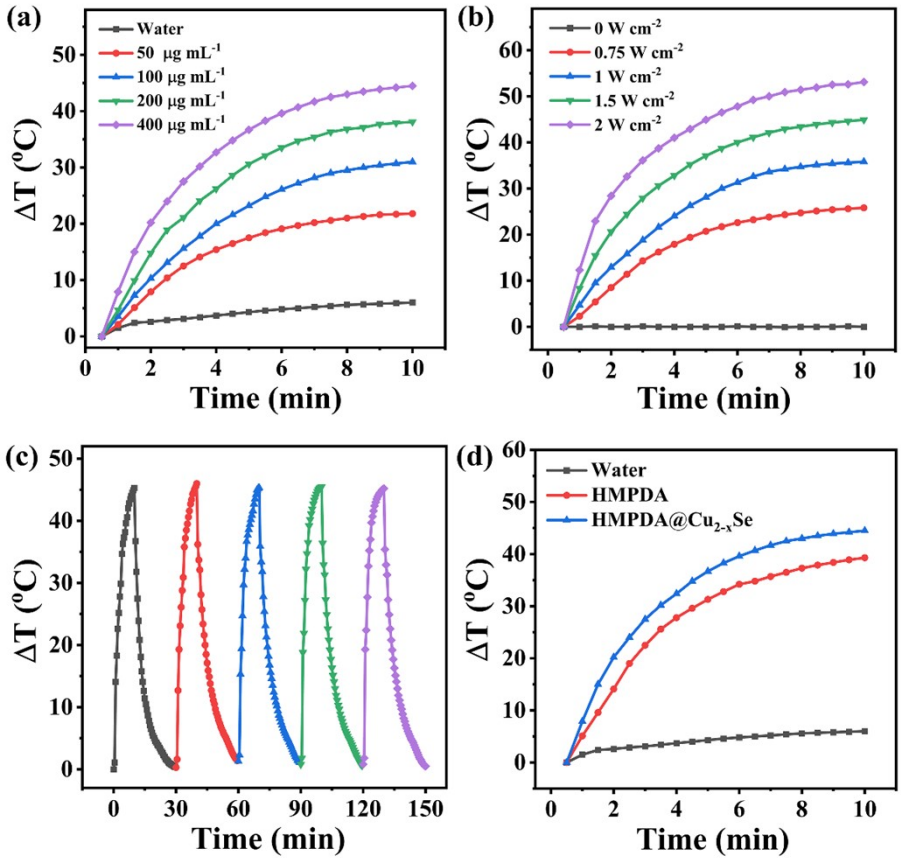

Fig. S3 (a) Concentration-dependent photothermal profiles of HMPDA@$Cu_{2-x}Se$ under 808 nm laser irradiation (1.0 W cm^{-2}); (b) Laser power density-dependent photothermal profiles of HMPDA@$Cu_{2-x}Se$ (HMPDA: 200 μg mL^{-1}); (c) Thermal cycle curves of HMPDA@$Cu_{2-x}Se$ (HMPDA: 200 μg mL^{-1}) under NIR laser irradiation (808 nm, 1.5 W cm^{-2}); (d) Temperature curves of water, and HMPDA@ $Cu_{2-x}Se$ (HMPDA: 200 μg mL^{-1}) under 808 nm laser irradiation (1.5 W cm^{-2}).

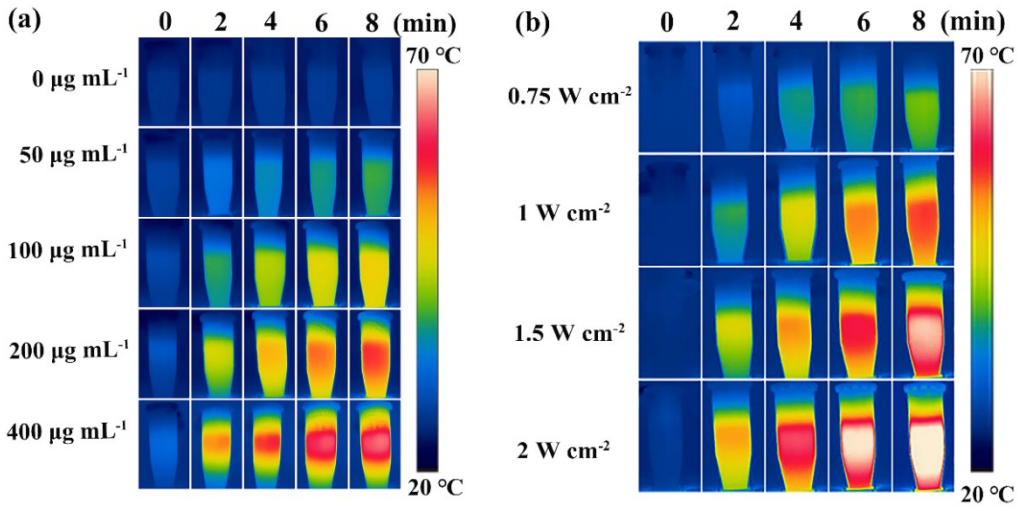

Fig. S4 Thermal images of HMPDA@$Cu_{2-x}Se$ aqueous solution at various concentrations (a) and powder density (b), respectively.

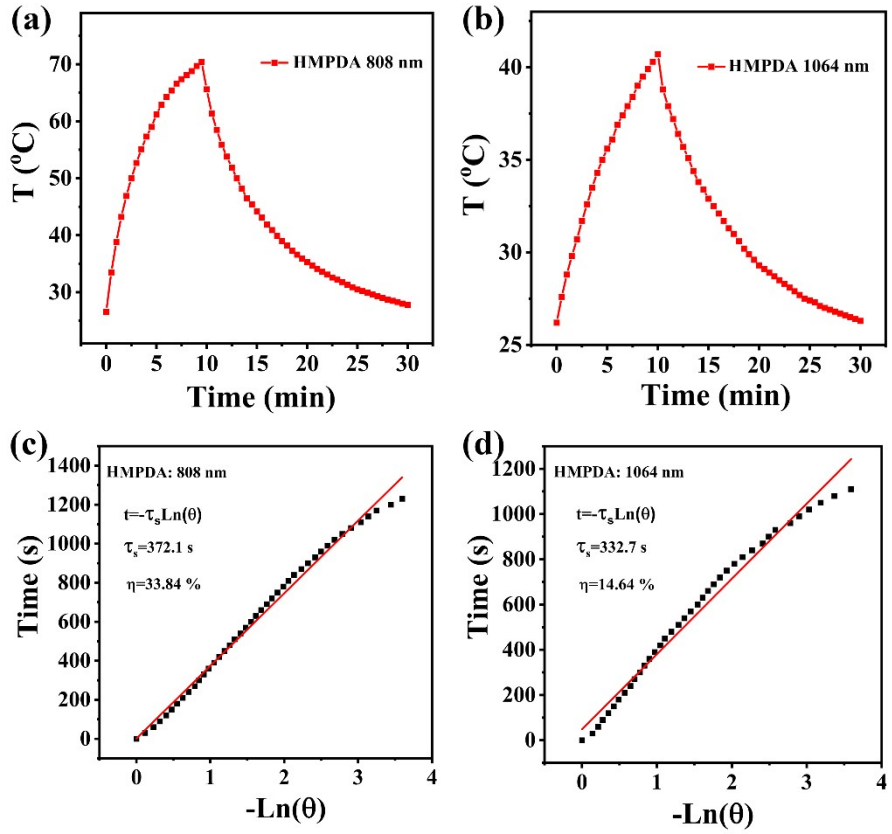

Fig. S5 Temperature curves of HMPDA aqueous solution (200 μg mL^{-1}) irradiated under 808 nm (a) and 1064 nm lasers (b) (1.5 W cm^{-2}); (c, d) Time constant for heat transfer obtained through the cooling period of (a, b), respectively.

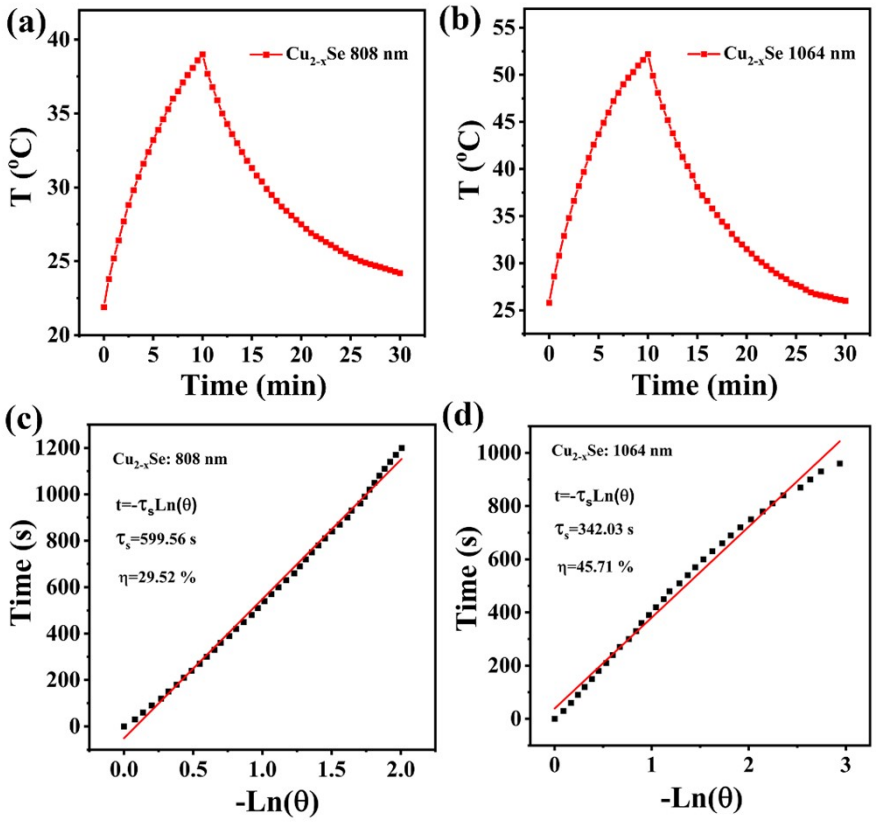

Fig. S6 Temperature curves of $Cu_{2-x}Se$ aqueous solution (50 μg mL^{-1}) irradiated under 808 nm (a) and 1064 nm lasers (b) (1.5 W cm^{-2}); (c, d) Time constant for heat transfer obtained through the cooling period of (a, b), respectively.

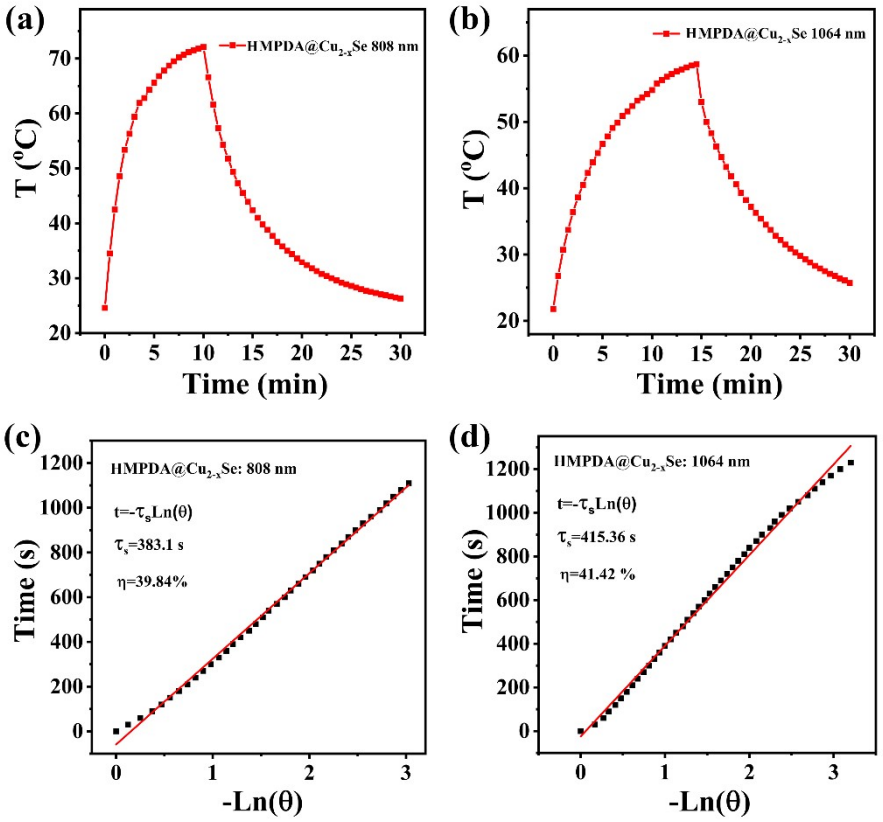

Fig. S7 Temperature curves of HMPC-D/G@PCM aqueous solution (MPDA: 200 μg mL^{-1}) irradiated under 808 nm (a) and 1064 nm lasers (b) (1.5 W cm^{-2}); (c, d) Time constant for heat transfer obtained through the cooling period of (a, b), respectively.

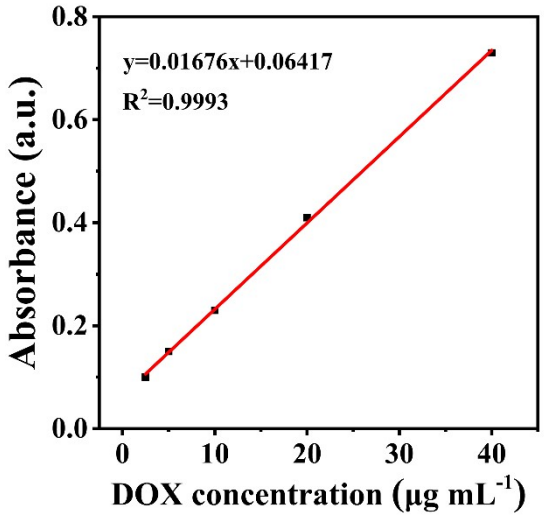

Fig. S8 Standard curves of DOX.

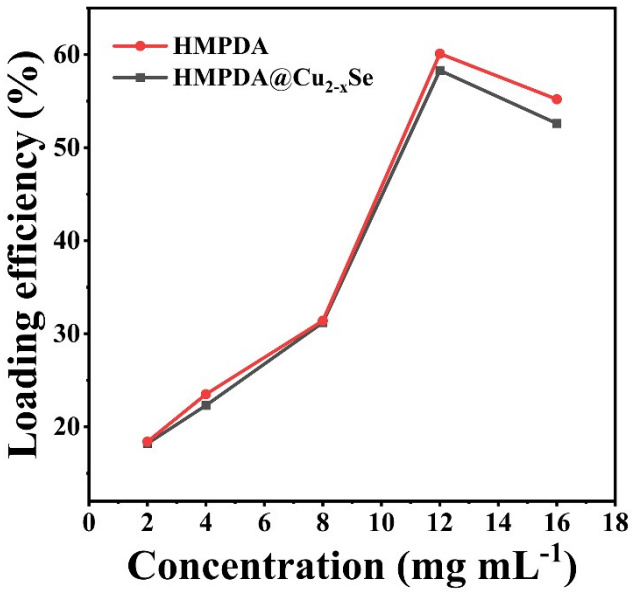

Fig. S9 DOX loading efficiency of HMPDA and HMPDA@$Cu_{2-x}Se$ (HMPDA: 4 mg mL^{-1}) versus various concentrations of DOX (2, 4, 8, 12 and 16 mg mL^{-1}).

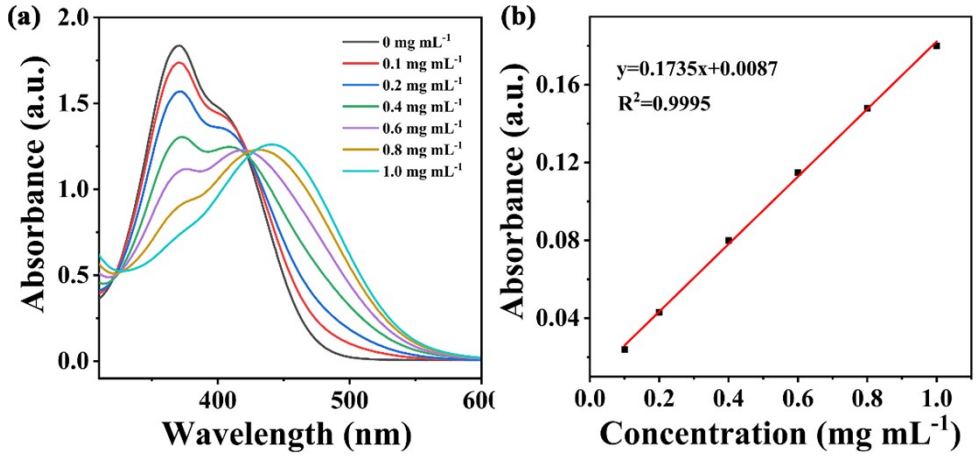

Fig. S10 (a) UV-Vis absorbance of glucose aqueous solution with different concentrations after treated by DNS reagent; (b) Corresponding standard curve of glucose.

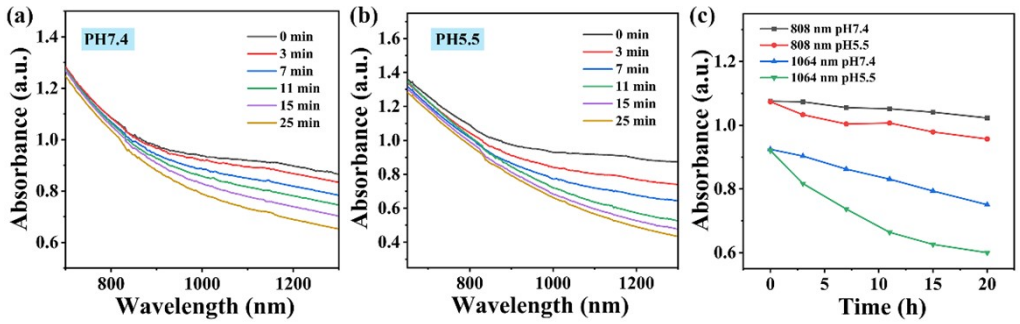

Fig. S11 Time-dependent UV-Vis-NIR absorbance spectra of HMPDA@$Cu_{2-x}Se$ in the aqueous solution containing H_2O_2 (10 mM) at pH 7.4 (a) and pH 5.5 (b), respectively; (c) Time-dependent changes of the absorbance intensity at 808 nm and 1064 nm in (a, b), respectively.

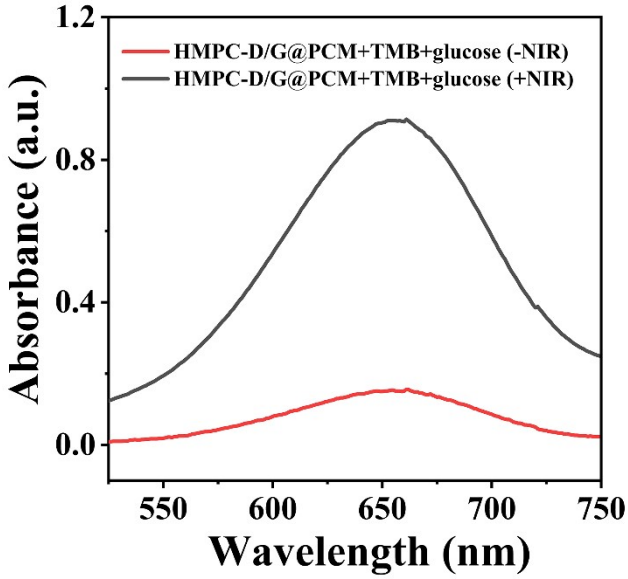

Fig. S12 Absorbance spectra of TMB oxidized by •OH radicals generated by the reactions of glucose (1 mg mL^{-1}) and HMPC-D/G@PCM (HMPDA: 400 μg mL^{-1}) without and with 1064 nm laser irradiation.

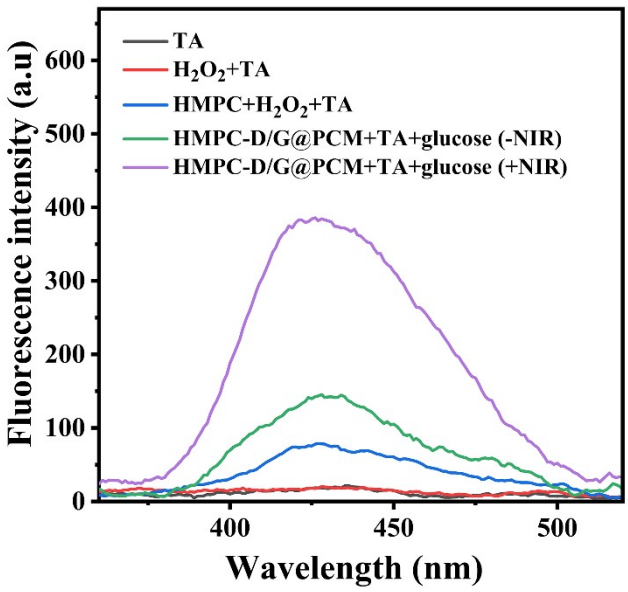

Fig. S13 Fluorescence spectra of terephthalate (TA) oxidized by •OH radicals generated from the reactions between HMPDA@$Cu_{2-x}Se$ (HMPC) and H_2O_2, and between HMPC-D/G@PCM and glucose with or without 1064 nm laser irradiation.

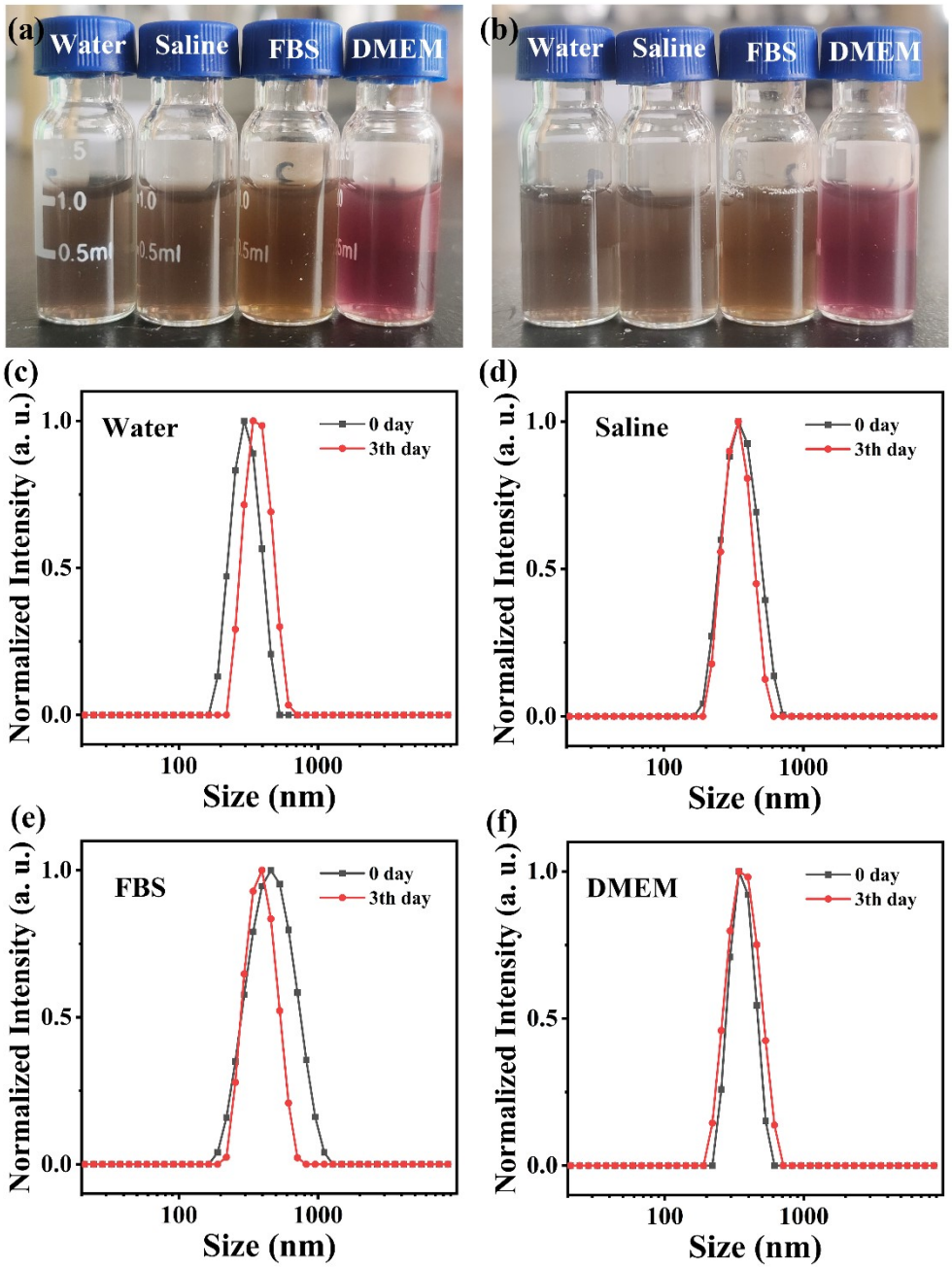

Fig. S14 Digital photographs (a: 0 day; b: 3th day) and corresponding hydrodynamic sizes (c-f) of HMPC-D/G@PCM dispersed in water, saline, fetal bovine serum (FBS), and DMEM for zero and three days, respectively.

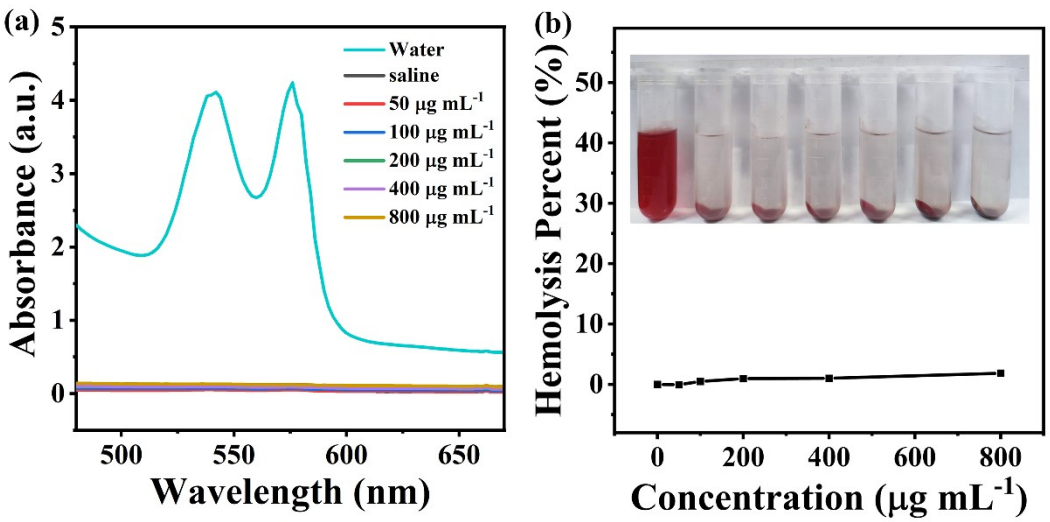

Fig. S15 (a) UV-Vis absorbance of the supernatants after incubating the HMPC-D/G@PCM nanomaterial with the red blood cells (RBC) of mice; (b) Hemolysis percentage of RBC at various concentrations of HMPC-D/G@PCM.

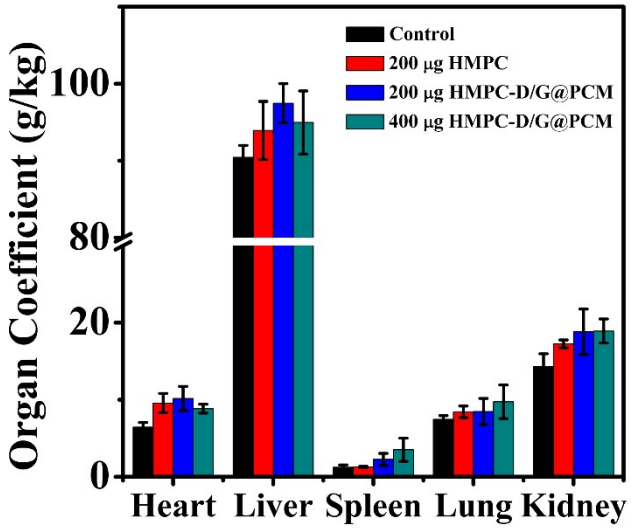

Fig. S16 Main organ coefficients of healthy mice injected with PBS, HMPDA@$Cu_{2-x}Se$ (HMPC, 200 μg), and different doses of HMPC-D/G@PCM (200, and 400 μg), respectively.

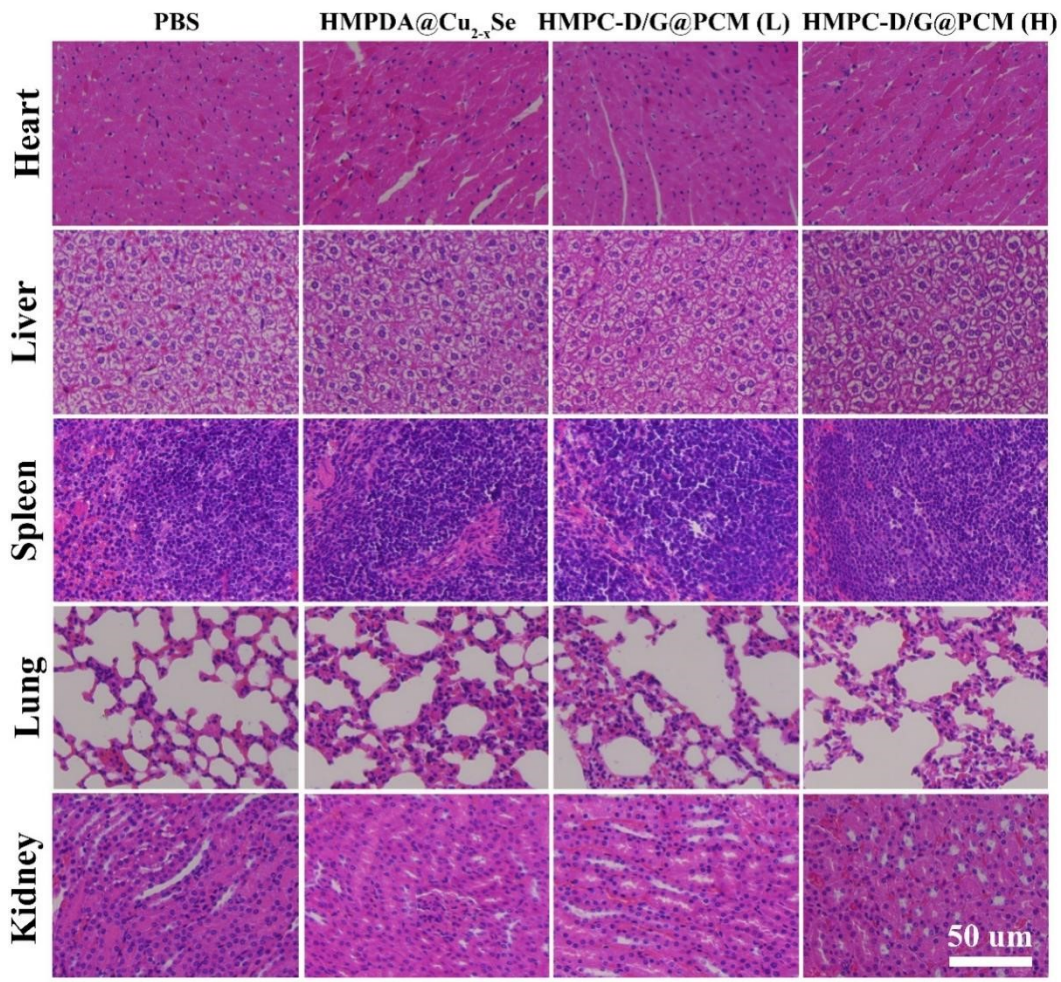

Fig. S17 H&E staining of the major organs of healthy mice injected with PBS, HMPDA@$Cu_{2-x}Se$ (HMPC, 200 μg), low dose (200 μg, denote as HMPC-D/G@PCM (L)), and high dose (400 μg, denote as HMPC-D/G@PCM (H)) of HMPC-D/G@PCM, respectively.

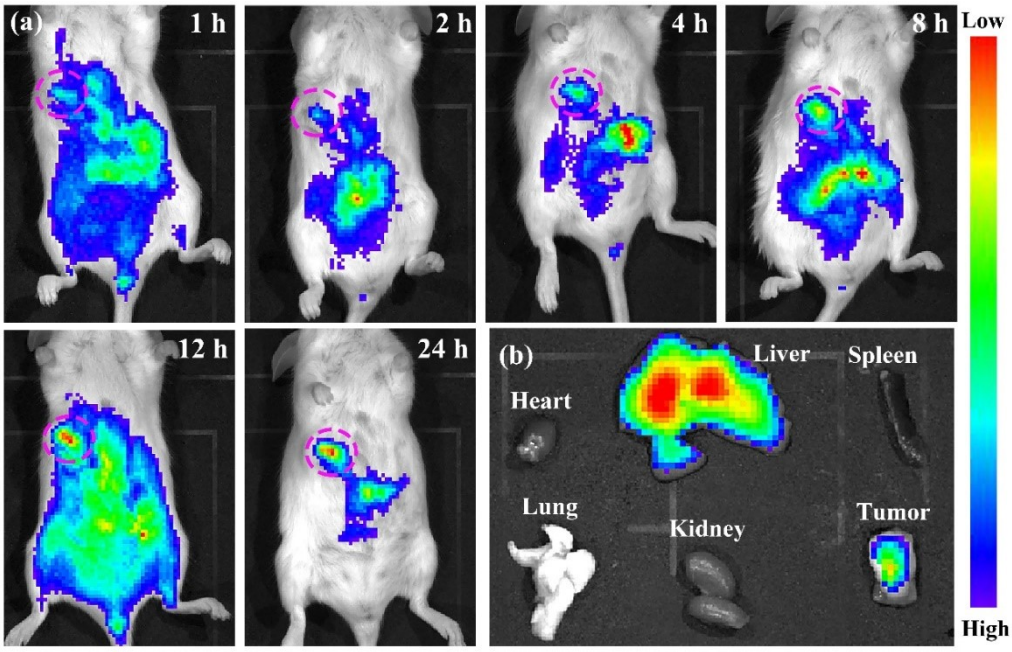

Fig. S18 (a) Time-dependent in vivo fluorescence imaging of mouse after intravenously injecting with NIR-797-labeled HMPDA@$Cu_{2-x}Se$; (b) Corresponding fluorescence image of tumors and major organs.

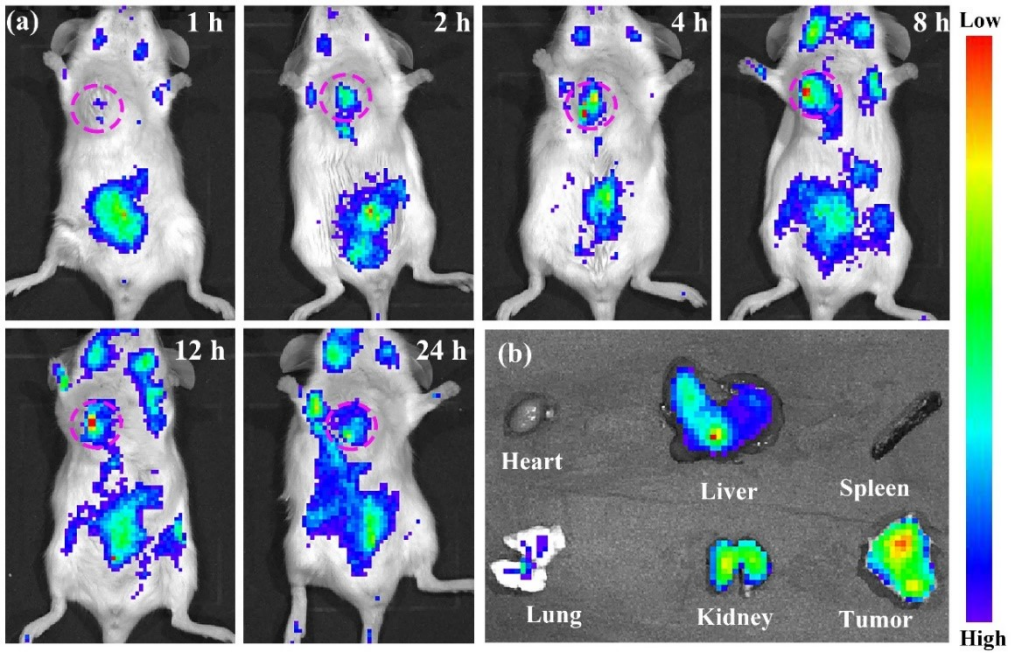

Fig. S19 (a) Time-dependent in vivo fluorescence imaging of mouse after intravenously injecting with NIR-797-labeled HMPC-D/G@PCM; (b) Corresponding fluorescence image of tumors and major organs.

Fig. S20 Digital photographs of mice in various groups after different treatments (Group 1: Control; 2: NIR; 3: GOx; 4: HMPDA@$Cu_{2-x}Se$; 5: HMPDA@$Cu_{2-x}Se$+NIR; 6: DOX; 7: HMPC-D/G@PCM; 8: HMPC-D@PCM+NIR; 9: HMPC-D/G@PCM+NIR).

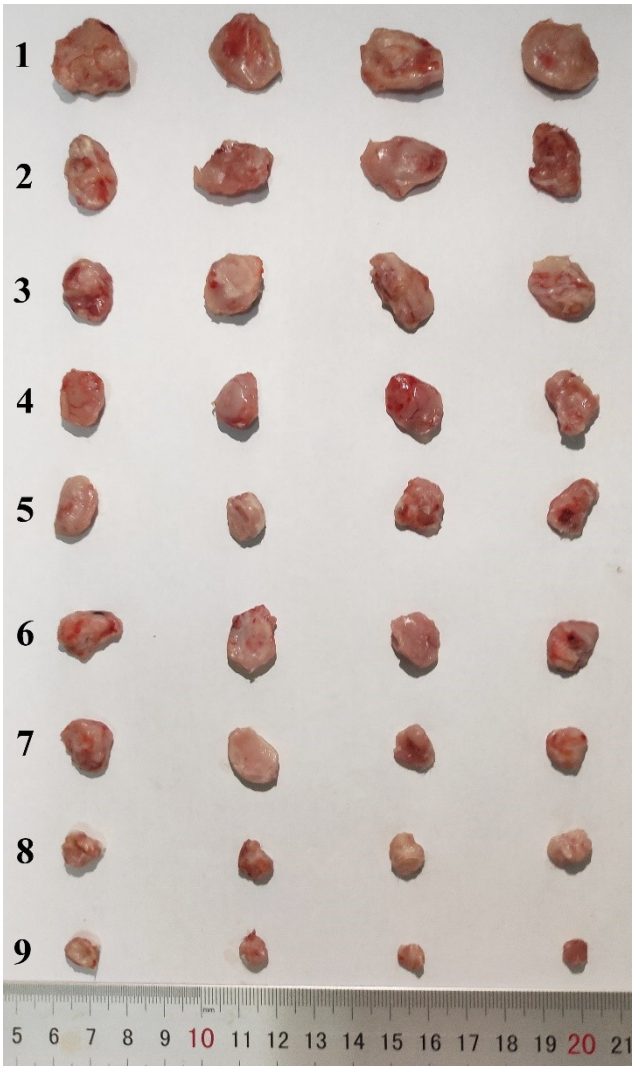

Fig. S21 Digital photographs of tumors in various groups after different treatments (Group 1: Control; 2: NIR; 3: GOx; 4: HMPDA@Cu2-xSe; 5: HMPDA@Cu2-xSe+NIR; 6: DOX; 7: HMPC-D/G@PCM; 8: HMPC-D@PCM+NIR; 9: HMPC-D/G@PCM+NIR).

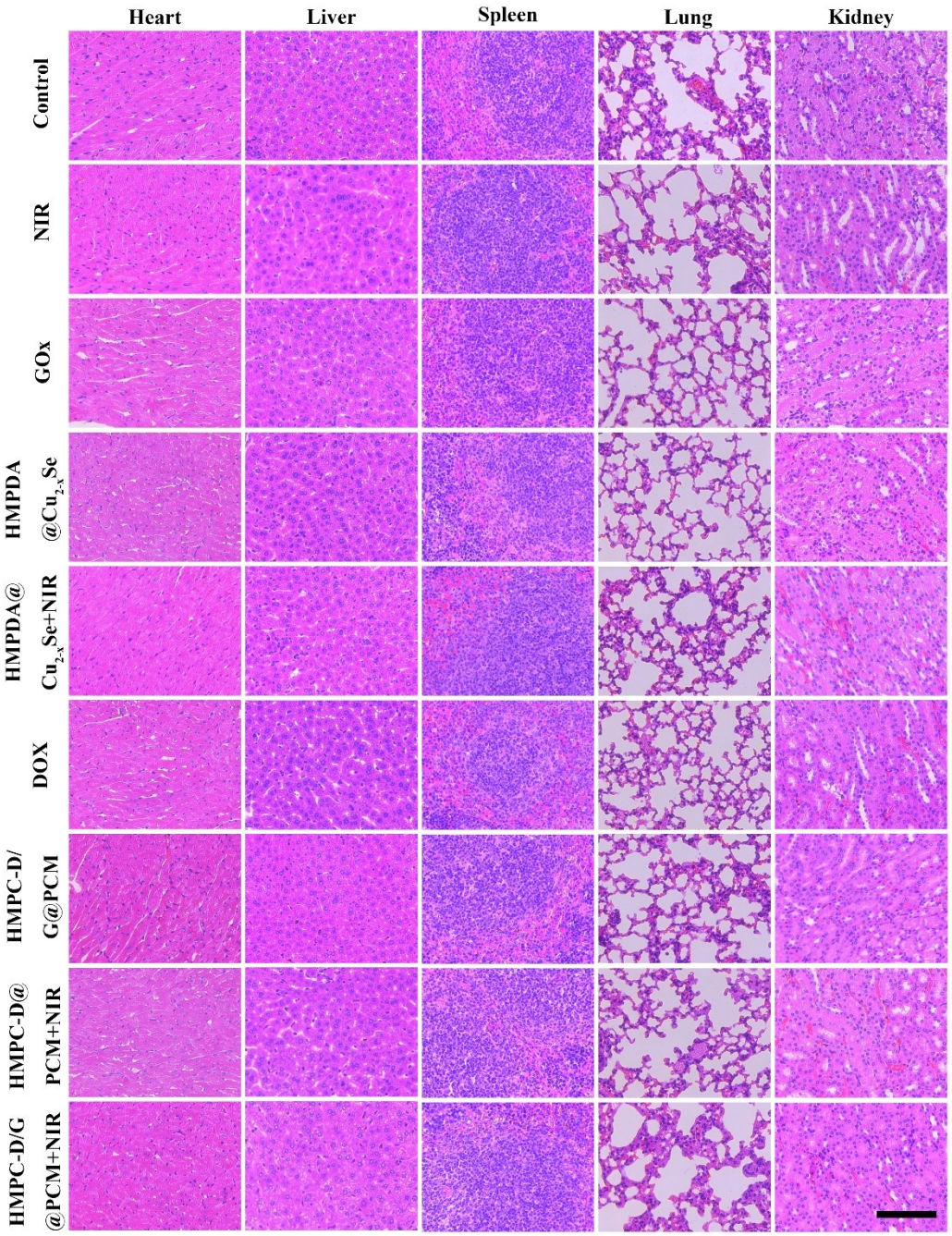

Fig. S22 H&E staining of the major organs after 14 days with different treatments. The scale bar is 50 μm.